HHS Public Access

Author manuscript

J Proteome Res. Author manuscript; available in PMC 2020 July 07.

Published in final edited form as:

J Proteome Res. 2020 April 03; 19(4): 1375–1382. doi:10.1021/acs.jproteome.9b00451.

Spatiotemporal proteomics reveals the molecular consequences of hormone treatment in a mouse model of lower urinary tract dysfunction

Samuel Thomas[1,#], **Ling Hao**[2,#], **Kellen DeLaney**[3], **Dalton McLean**[4], **Laura Steinke**[2], **Paul C. Marker**[2], **Chad M. Vezina**[1,5,6], **Lingjun Li**[1,2,3,*], **William A. Ricke**[1,2,4,5,*]

[1]Molecular and Environmental Toxicology Center, University of Wisconsin-Madison, Madison, WI, USA

[2]School of Pharmacy, University of Wisconsin-Madison, Madison, WI, USA

[3]Department of Chemistry, University of Wisconsin-Madison, Madison, WI, USA

[4]Department of Urology, University of Wisconsin-Madison, Madison, WI, USA

[5]George M. O'Brien Center of Research Excellence, University of Wisconsin-Madison, Madison, WI, USA

[6]School of Veterinary Medicine, University of Wisconsin-Madison, Madison, WI, USA

Abstract

Benign prostatic hyperplasia and related lower urinary tract symptoms remain common, costly, and impactful issues for aging males. Etiology and pathogenesis are multifactorial and include steroid hormone changes and inflammation. Noninvasive markers could one day inform personalized medicine, but interindividual variation and lack of healthy age-matched controls hamper research. Experimental models are appealing for insight into disease mechanisms. Here, we present a spatiotemporal proteomics study in a mouse model of hormone-induced urinary dysfunction. Urine samples were collected noninvasively across time: before, during, and after disease onset. Microcomputed tomography analysis implicated the prostate as a spatially relevant contributor to bladder outlet obstruction. Prostates were collected after disease onset and compared with control mice. Notable changes in urine include proteins representing oxidative stress defense and acute phase inflammatory response processes. In the prostate, hormone treatment led to perturbations related to oxidative stress response and H_2O_2 metabolism. Several protein changes coincided in both urine and prostate tissue, including GPX3, GGT1, and GC. This

[*]Corresponding authors contributed equally to this work. Tel.: +1 (608)265-8491; +1 (608) 265-3202, lingjun.li@wisc.edu; rickew@urology.wisc.edu.

[#]Contributed equally to this work.

DATA DEPOSITION

The mass spectrometry proteomics data have been deposited to the ProteomeXchange Consortium via the PRIDE partner repository [44] with the dataset identifier PXD014416.

ASSOCIATED CONTENT

The following supporting information is available free of charge at ACS website http://pubs.acs.org

CONFLICT OF INTEREST DISCLOSURE

The authors declare no competing financial interests.

study supports the concept of noninvasive urinary biomarkers for prostate disease diagnostics. Oxidative stress and acute phase inflammatory processes were identified as key consequences of hormone-induced bladder outlet obstruction. Future research into antioxidants and anti-inflammatories in prostate disease appears promising.

Graphical Abstract

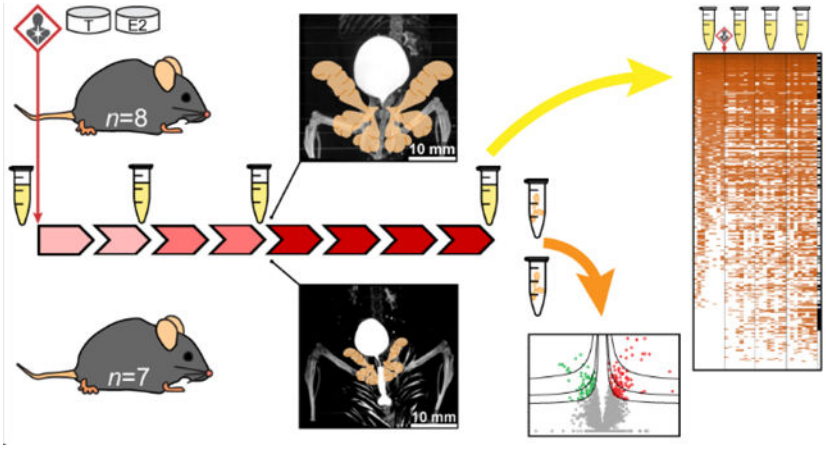

Keywords

spatiotemporal; proteomics; endocrine disruption; urine; prostate; lower urinary tract symptoms

INTRODUCTION

Lower urinary tract symptoms (LUTS) are often accompanied by benign prostatic hyperplasia (BPH) and occur at a high rate in aging males, with substantial cost (>$3.9 B/yr in US) [1] and detriment to quality of life [2]. These symptoms include painful or frequent urination, nocturia and sleep disturbance, and acute urinary retention, which can prove fatal [3]. The etiology of BPH/LUTS is multifactorial and likely includes changes in steroid hormones associated with aging or environmental exposures, inflammation, oxidative stress, and metabolic disease [4–6]. An important pathogenesis, urethral occlusion secondary to BPH, is associated with fibrosis, smooth muscle dysfunction, and hyperplasia [7]. Diagnosis of LUTS remains subjective – based on patient symptom surveys [8]. Surgical interventions are common, as efficacy and tolerance of current drugs are imperfect [9]. We and others have investigated possible noninvasive urinary biomarkers, with the goals of stratifying patients for personalized medicine and identifying potential druggable pathways for new therapeutics [10–12], but more work is needed to validate and link these with disease subtypes. Mouse models of disease could provide valuable mechanistic insight, owing to inherently low interindividual variability and tightly controlled experimental conditions.

Aging males experience BPH/LUTS concurrent with a decreasing testosterone:estradiol ratio. Furthermore, when age is controlled-for, decreased testosterone:estradiol ratio associates with LUTS [13], prostate inflammation [14], and BPH [15, 16] – indicating a potential role for this endocrine disruption in disease etiology. Aging-associated changes in plasma

steroid hormone concentrations are subtle [17, 18] and environmental endocrine disruptors appear capable of generating similar effects [19, 20], but more work is needed to fully appreciate the role of hormones and endocrine disruption in BPH/LUTS. Therapies that antagonize or selectively modulate estrogen receptors or downstream signaling processes appear promising for BPH/LUTS treatment or prevention [21, 22].

The present study employed a human-relevant mouse model of lower urinary tract dysfunction, which relies on slow-release, subcutaneous hormone implants to generate marked bladder outlet obstruction by as early as 4 weeks of exposure [23]. The urologic effects of this model are well-characterized [23–25], and prior work demonstrated that estrogen receptor alpha is necessary for bladder outlet obstruction [23], but little else is known about the molecular signature associated with urinary dysfunction. To learn more about the molecular underpinnings of hormone-induced bladder outlet obstruction, we undertook a spatiotemporal proteomics experiment (Fig. 1). Here, noninvasive urine sampling before, during, and after the onset of bladder outlet obstruction allowed temporal monitoring via global proteomics in treated mice. Spatial proteomics of treated and untreated mouse prostates provided insight into the potential source of changes observed in urine – a validation step often obviated by limited patient tissue availability in benign diseases like BPH/LUTS. Prostate tissue proteomics also provides a more comprehensive view into disease processes occurring at the site of bladder outlet obstruction.

EXPERIMENTAL SECTION

Mouse Treatment

All animal experiments and procedures were conducted under protocols approved by the University of Wisconsin Animal Care and Use Committee. Eighteen adult male C57BL/6 mice were used in this study (Charles River, Wilmington, MA). Nine received slow-release, subcutaneous hormone pellet implants of 2.5 mg 17β-estradiol (with 22.5 mg cholesterol binder) and 25 mg testosterone (Fig. 1), as previously described [24]. Nine untreated mice served as age-matched littermate controls for the tissue-based analyses. All mice were maintained under standard laboratory conditions throughout the experiment (12-hr light/12hr dark cycle; Teklad 8604 food and water *ad libitum*). One mouse per group was used for a terminal microcomputed tomography imaging experiment at the week 4 time point.

Sample Collection and Preparation

Urine Samples—Mouse urine was collected before hormone pellet implantation (week 0) and after 2, 4, and 8 weeks of this treatment via metabolic cage ($n = 8$). Urine sampling occurred at the same time during the morning of each time point. Urine deposited in the cage (500 μL) was preserved with 4% sodium azide (*v/v*), frozen on dry ice, and stored at −80 °C until further processing.

Urine samples were prepared for global proteomic analysis via urea in-solution trypsin digestion. Briefly, urine samples were thawed on ice, vortexed to redissolve protein, and aliquoted into a 3 kDa centrifugal filter device (Millipore, Burlington, MA). The retained protein fraction (> 3 kDa) was obtained following the manufacturer's protocol. Proteins

were quantified via BCA assay (Thermo, Waltham, MA) and 20 μg were digested as follows. Lyophilized proteins were redissolved in 8 M urea / 50 mM Tris buffer (pH = 8), disulfide bonds were reduced with 5 mM dithiothreitol (DTT) for 1 hr, free thiol groups were alkylated with 15 mM iodoacetamide for 30 min (dark), and the reaction was quenched via 5 mM DTT. Samples were then diluted to <1 M urea via 50 mM Tris buffer and digested with sequencing-grade trypsin (Promega, Madison, WI) at 50:1 (protein:enzyme) for 18 hours at 37 °C. Tryptic peptides were desalted via C18 OMIX pipette tips (Agilent, Santa Clara, CA) before lyophilization and storage at −80 °C until analysis.

Prostate Tissue Samples—Treated (n = 8) and untreated (n = 8) mice were sacrificed after the week 8 urine collection time point. Mice were euthanized by CO_2 asphyxiation and each mouse was analyzed as a single biological unit. Bladder and prostate masses were recorded. Half of the anterior, ventral, and dorsolateral prostate lobes were combined into a single tube, frozen on dry ice, and stored at −80 °C until further processing.

Prostate tissue samples were prepared for global proteomics analysis via a modified surfactantaided sample preparation technique with trypsin, as previously described [26]. Briefly, frozen prostates were thawed and homogenized in a solution containing sodium dodecyl sulfate, deoxycholic acid, and a reducing agent in an ammonium bicarbonate buffer. Aliquots of homogenate were added to pre-passivated 30 kDa centrifugal filter units (Millipore, Burlington, MA) for urea buffer exchange and alkylation, followed by 18-hour digestion with sequencing-grade trypsin (Promega, Madison, WI), and final collection of peptides. Samples were cleaned up via SCX spin tips (Protea Biosciences, Morgantown, WV), followed by desalting with C18 OMIX pipette tips (Agilent, Santa Clara, CA), and peptide quantification via BCA assay (Thermo, Waltham, MA). Lyophilized peptides were stored at −80 °C until analysis.

Microcomputed Tomography Procedure

Prior studies have demonstrated marked hormone-induced bladder outlet obstruction by 4 weeks of treatment [23]. To provide additional temporal evidence for the onset of bladder outlet obstruction, and to more accurately visualize the location and severity of bladder outlet obstruction after 4 weeks of treatment, we imaged the lower urinary tracts of one treated and one untreated mouse *in situ* via microcomputed tomography (μCT).

Mice were prepared and imaged as follows. Intraperitoneal saline (1 mL) and tail-vein ISOVUE370 contrast agent (0.25 mL) were administered 15 minutes prior to euthanasia by sodium pentobarbital. Mice were imaged at the University of Wisconsin – Madison Small Animal Imaging Facility on a Siemens Inveon μCT instrument for 20 minutes at a resolution of 20 μm. Three-dimensional reconstruction of images was achieved using Siemens Inveon Research software.

Mass Spectrometry

Mass spectrometry-based, label-free global proteomics with relative quantification was used to assess protein-level changes in urine and prostate tissue samples due to hormone treatment. All samples were analyzed on a Thermo Dionex nanoLC system coupled to a

Thermo Q Exactive HF mass spectrometer. A C18 column was fabricated in-house with an integrated electrospray ionization emitter (75.1 μm × 150 mm, BEH 1.7 μm, 130 Å). Samples were kept at 4 °C in the autosampler. Mobile phase A was 0.1% formic acid in H_2O and mobile phase B was 0.1% formic acid in acetonitrile (Fisher, Hampton, NH). Flow rate was 0.3 μL/min. The nanoLC gradient was as follows: 0–16 min 3% B, 16–106 min 3–30% B (linear), 106106.5 min 30–75% B (linear), 106.5–116 min 75% B, 116–116.5 min 75–95% B (linear), 116.5–126 min 95% B, 126–126.5 min 95–3% B (linear), 126.5–141 min 3% B. Top 15 data-dependent acquisitions were conducted with the full MS scanned from *m/z* 300–1,500 at a resolving power of 60K (at *m/z* 200) and an S-lens radio frequency of 30. Parent masses were isolated in the quadrupole with an isolation window of 1.4 *m/z* and fragmented with higher-energy collisional dissociation with a normalized collision energy of 30 eV. MS/MS scans were detected in the Orbitrap using the rapid scan rate, a dynamic exclusion time of 45 s, and a resolution of 15K (at *m/z* 200). Automatic gain control targets were 3×10^6 for MS and 1×10^5 for MS/MS acquisitions. Maximum injection times were 50 ms for MS and 100 ms for MS/MS.

Data Processing and Statistical Analysis

Protein identification and relative quantification for urine and prostate samples were achieved using MaxQuant software (v1.6.2.10; Max Planck Institute, Martinsried, Germany) [27], with protein- and peptidelevel FDR = 0.01, match between runs, intensity-based absolute quantification, manual mean normalization, and the Swiss-Prot *Mus musculus* database (v2018_11). Urine and prostate samples were processed in separate batches.

Significant changes in bladder and prostate mass were determined using the Student's *t*-test after $\log_2$ normalization ($\alpha = 0.05$; GraphPad Prism v5.04, La Jolla, CA). Significant changes in urine proteins across time were determined using the repeated measures-analysis of variance (RM-ANOVA) with Tukey's post-hoc test after $\log_2$ normalization ($\alpha = 0.05$; Java, Redwood Shores, California). Process-level roles for significant proteins were determined manually using the UniProt and GeneCards online databases. Significant changes in prostate tissue proteomics were determined via volcano plot using Student's *t*-test and a permutation-based FDR ($\alpha = 0.05$; Perseus v1.6.2.3; Max Planck Institute, Martinsried, Germany) [28]. Significantly overrepresented biological processes in the prostate proteomics dataset were determined using the Hypergeometric test with Benjamini & Hochberg FDR correction ($\alpha = 0.05$; BiNGO tool, Cytoscape v3.6.1) [29, 30].

RESULTS AND DISCUSSION

Morphometrics

Microcomputed tomography imaging provided noninvasive, *in situ* visualization of a urinary occlusion located in the area of the prostate after 4 weeks of hormone treatment ($n = 1$ treated *vs* $n = 1$ control) (Fig. 1, Fig. S-4). In an unobstructed control mouse, contrast is present throughout the urethra, continuing externally to the fur. Hormone treatment led to apparent urinary retention and bladder enlargement. As expected, bladder and prostate masses after 8 weeks of treatment were significantly different and increased with treatment ($n = 8$ treated *vs* $n = 8$ control; Student's *t*-test, $\alpha = 0.05$) (Fig. 1).

Urinary Proteomics – Across Time

Urinary proteomics identified 338 total proteins, with 120 demonstrating a significant change in at least one time point ($n = 8$; RM-ANOVA, Tukey's post-hoc) (Fig. 2, Table S-1). Notably, several of these proteins play critical roles in oxidative stress defense and were generally increased throughout disease onset (Fig. 3). Additionally, several proteins of the acute phase inflammatory response and xenobiotic response also demonstrated significant changes throughout disease onset, and were generally increased across time (Fig. S-1). Proteins representing these processes that did not generally increase across time include VWA3A (Fig. S-1), which decreased and rebounded, and SERPINA1E (Fig. S-1), which fell below detection coincident with the arrival of SERPINB1A (Fig. S-1). Other proteins with known immunologic roles and proteins related to blood and iron were also among these significant changes (Fig. S-2, Fig. S-3). Oxidative stress can lead to innate immune response via damage-associated molecular pattern signaling [31, 32] and may underlie bladder outlet obstruction in this model. Oxidative stress and inflammation have long been associated with LUTS and prostate disease [33, 34], but the role of steroid hormones in these processes remains to be explored. Of note, the source of protein changes observed in urine is often unclear and could include systemic circulation, prostatic secretions, kidneys, and bladder [35]. Tissue-specific genetic manipulation [36], tissue-specific proteins, or orthogonal tissue analyses can help shed light on the origin of urine protein changes.

Prostate Proteomics – Site of Bladder Occlusion

The prostate is an important contributor to LUTS in patients and was spatially implicated in bladder outlet obstruction here via μCT. Prostate proteomics identified 3849 proteins and 115 were significantly modulated with hormone treatment ($n = 8$ treated *vs* $n = 7$ control; Student's *t*-test, permutation-based FDR = 0.15) (Fig. 4, Tables S-2 and S-3). Gene ontology analysis identified significantly overrepresented processes consistent with those observed in urine: oxidative stress response, hydrogen peroxide (H_2O_2) metabolism, and nucleobase salvage (Hypergeometric test with B & H FDR, $\alpha = 0.05$) (Fig. 4). Other processes with potential relevance in LUTS include neural development and mitogen-activated protein kinase activity. Some processes appear to be hormone-relevant, but the connection to prostate disease is unclear: male courtship and mating behavior, mating plug formation, among others (Fig. 4, Fig. S-5). Future tissue proteomics efforts focusing on the prostatic urethra, perhaps using laser capture microdissection and multiple time points, could further describe the molecular consequences of hormone treatment in this model.

Putative Urinary Biomarkers of Prostate Disease

One hundred ninety-eight proteins identified in prostate tissue were also found in urine (Fig. 5). Thirty-four of these changed significantly in prostate and 15 displayed significant modulation in both prostate tissue and urine – making these potential urinary biomarkers of hormone treatment in the prostate (Table 1). Several putative biomarkers displayed strong fidelity with respect to the direction and magnitude of changes in prostate and urine (Table 1). Apparent discrepancies may relate to the timing of sampling with this study design, where significant differences could exist between any of 4 points across 8 weeks in urine, but just the 8-week time point in prostate tissues. Future studies at earlier time points in

prostate could clarify these tissue-level temporal changes. Other proteins of potential interest include PSCA, PIGR, and CTSB, as these were significantly modulated in prostate tissue, and had *p*-values < 0.15 in urine, but did not reach significance at $p = 0.05$ (RM-ANOVA) (Tables S-1 and S-3).

Taken together, these data suggest oxidative stress leading to innate immune response may underlie hormone-induced bladder outlet obstruction in this mouse model. These findings are consistent with known BPH/LUTS disease processes in humans and with previous mechanistic reports regarding the effects of hormones on the prostate in murine models. A previous urinary proteomics analysis comparing patients with LUTS to age-matched controls identified significantly overrepresented processes related to the acute inflammatory and innate immune responses [10] (Fig. S-6). Others have also shown associations between oxidative stress and inflammation and BPH/LUTS [33, 34]. Additionally, prior reports suggest estrogen is pro-inflammatory in the prostate: both exogenous E_2 in rats [37, 38] and increased endogenous E_2 in mice [39]. Furthermore, co-administration with an antioxidant can prevent hormone-induced prostatic inflammation in the rat [40]. Interestingly, the pro-inflammatory effects of E_2 may be abrogated by the 12-week time point [41]. Future work will explore the mechanism of hormone-induced inflammation and potential interventions (*e.g.* selective estrogen receptor modulators and antagonists).

Proteome coverage here was sufficient to identify significantly modulated proteins in both urine and prostate tissue, including coinciding proteins that represent interesting biological processes with precedence in the human disease (*e.g.* oxidative stress and inflammation). However, upstream separation strategies would likely increase the depth of proteome coverage, particularly for proteins of low abundance in urine. Mouse urine contains several classes of high-abundance proteins, which were observed in the present study (*e.g.* major urinary proteins (MUPs)), and can serve to suppress ionization or bias data-dependent acquisitions against low-abundance peptides [35]. Examples of strategies that could improve urine proteome coverage include extensive sample prefractionation [42] and two-dimensional chromatography techniques [43]. Additionally, future research focused on the translational aspect of hormone-related LUTS (*e.g.* stratification of BPH/LUTS for personalized medicine) will require carefully recruited patient groups, ideally with matched biopsy-biofluid samples.

CONCLUSION

Hormone treatment leads to bladder outlet obstruction in this mouse model and the prostate is a likely contributor, but the molecular consequences were largely unknown. This spatiotemporal proteomics study demonstrates that hormone treatment leads to a number of protein-level changes within the mouse prostate related to known BPH/LUTS disease processes, such as oxidative stress defense and the innate immune response. Furthermore, many of these tissue-level proteomic changes coincide in urine and can be noninvasively monitored there across time. Future research into therapies targeting these processes (*e.g.* antioxidants and anti-inflammatories) or upstream hormone signaling (*e.g.* selective estrogen receptor modulators) in BPH/LUTS appears promising. Additionally, this study supports the

concept of noninvasive urine biomarkers of prostatic disease, which could allow patient stratification and personalized medicine.

Supplementary Material

Refer to Web version on PubMed Central for supplementary material.

ACKNOWLEDGMENTS

The authors acknowledge Seth Hyman for assistance with sample collection. ST acknowledges an NIHsupported Molecular and Environmental Toxicology Training Program Predoctoral Fellowship (grant number T32-ES007015). KD acknowledges the National Institutes of Health-General Medical Sciences F31 National Research Service Award (1F31GM126870-01A1) for funding. LL acknowledges a Vilas Distinguished Achievement Professorship with funding provided by the Wisconsin Alumni Research Foundation and University of Wisconsin-Madison School of Pharmacy. This work was also supported by National Institutes of Health through grants P30 CA014520, P20 DK097826, NIH/NIDDK U54 DK104310, NIH R01 ES01332 (CMV and WAR), NIH R01 DK071801, and NIH P41GM108538 (LL). The Orbitrap instruments were purchased through the support of an NIH shared instrument grant (NIH-NCRR S10RR029531).

REFERENCES

1. Saigal CS; Joyce G, Economic costs of benign prostatic hyperplasia in the private sector. J Urol 2005, 173, (4), 1309–13. [PubMed: 15758787]
2. Robertson C; Link CL; Onel E; Mazzetta C; Keech M; Hobbs R; Fourcade R; Kiemeney L; Lee C; Boyle P; McKinlay JB, The impact of lower urinary tract symptoms and comorbidities on quality of life: the BACH and UREPIK studies. BJU Int 2007, 99, (2), 347–54. [PubMed: 17313423]
3. Wei JT; Calhoun E; Jacobsen SJ, Urologic diseases in America project: benign prostatic hyperplasia. J Urol 2005, 173, (4), 1256–61. [PubMed: 15758764]
4. Kramer G; Mitteregger D; Marberger M, Is Benign Prostatic Hyperplasia (BPH) an Immune Inflammatory Disease? European Urology 2007, 51, (5), 1202–1216. [PubMed: 17182170]
5. Vital P; Castro P; Ittmann M, Oxidative stress promotes benign prostatic hyperplasia. Prostate 2016, 76, (1), 58–67. [PubMed: 26417670]
6. Gacci M; Vignozzi L; Sebastianelli A; Salvi M; Giannessi C; De Nunzio C; Tubaro A; Corona G; Rastrelli G; Santi R; Nesi G; Serni S; Carini M; Maggi M, Metabolic syndrome and lower urinary tract symptoms: the role of inflammation. Prostate Cancer Prostatic Dis 2013, 16, (1), 101–6. [PubMed: 23165431]
7. Rodriguez-Nieves JA; Macoska JA, Prostatic fibrosis, lower urinary tract symptoms, and BPH. Nature Reviews Urology 2013, 10, (9), 546–550. [PubMed: 23857178]
8. Novara G; Galfano A; Gardi M; Ficarra V; Boccon-Gibod L; Artibani W, Critical Review of Guidelines for BPH Diagnosis and Treatment Strategy. European Urology Supplements 2006, 5, (4), 418–429.
9. Oelke M; Bachmann A; Descazeaud A; Emberton M; Gravas S; Michel MC; N'Dow J; Nordling J; de la Rosette JJ; European Association of U, EAU guidelines on the treatment and follow-up of non-neurogenic male lower urinary tract symptoms including benign prostatic obstruction. Eur Urol 2013, 64, (1), 118–40. [PubMed: 23541338]
10. Greer T; Hao L; Nechyporenko A; Lee S; Vezina CM; Ricke WA; Marker PC; Bjorling DE; Bushman W; Li L, Custom 4-Plex DiLeu Isobaric Labels Enable Relative Quantification of Urinary Proteins in Men with Lower Urinary Tract Symptoms (LUTS). PLoS One 2015, 10, (8), e0135415.
11. Hao L; Greer T; Page D; Shi Y; Vezina CM; Macoska JA; Marker PC; Bjorling DE; Bushman W; Ricke WA; Li L, In-Depth Characterization and Validation of Human Urine Metabolomes Reveal Novel Metabolic Signatures of Lower Urinary Tract Symptoms. Scientific Reports 2016, 6, (1), 30869–30869. [PubMed: 27502322]
12. Mitsui T; Kira S; Ihara T; Sawada N; Nakagomi H; Miyamoto T; Shimura H; Yokomichi H; Takeda M, Metabolomics Approach to Male Lower Urinary Tract Symptoms: Identification of Possible

Biomarkers and Potential Targets for New Treatments. J Urol 2018, 199, (5), 1312–1318. [PubMed: 29175111]

13. Rohrmann S; Nelson WG; Rifai N; Kanarek N; Basaria S; Tsilidis KK; Smit E; Giovannucci E; Platz EA, Serum sex steroid hormones and lower urinary tract symptoms in Third National Health and Nutrition Examination Survey (NHANES III). Urology 2007, 69, (4), 708–13. [PubMed: 17445656]
14. Condorelli RA; Calogero AE; La Vignera S, Hyperestrogenism and low serum testosterone-17beta-estradiol ratio are associated with non-bacterial male accessory gland inflammation. Int J Immunopathol Pharmacol 2016, 29, (3), 488–93. [PubMed: 27091838]
15. Ortega E; Ruiz E; Mendoza M; Martin-Andres A; Osorio C, Plasma steroid and protein hormone concentrations in patients with benign prostatic hypertrophy and in normal men. Experientia 1978, 35, (6), 844–845.
16. Prins GS; Korach KS, The role of estrogens and estrogen receptors in normal prostate growth and disease. Steroids 2008, 73, (3), 233–44. [PubMed: 18093629]
17. Juul A; Skakkebaek NE, Androgens and the ageing male. Hum Reprod Update 2002, 8, (5), 423–33. [PubMed: 12398223]
18. Harman SM; Metter EJ; Tobin JD; Pearson J; Blackman MR; Baltimore Longitudinal Study of, A., Longitudinal effects of aging on serum total and free testosterone levels in healthy men. Baltimore Longitudinal Study of Aging. J Clin Endocrinol Metab 2001, 86, (2), 724–31. [PubMed: 11158037]
19. Joensen UN; Veyrand B; Antignac JP; Blomberg Jensen M; Petersen JH; Marchand P; Skakkebaek NE; Andersson AM; Le Bizec B; Jorgensen N, PFOS (perfluorooctanesulfonate) in serum is negatively associated with testosterone levels, but not with semen quality, in healthy men. Hum Reprod 2013, 28, (3), 599–608. [PubMed: 23250927]
20. Zhou Y; Hu LW; Qian ZM; Chang JJ; King C; Paul G; Lin S; Chen PC; Lee YL; Dong GH, Association of perfluoroalkyl substances exposure with reproductive hormone levels in adolescents: By sex status. Environ Int 2016, 94, 189–195. [PubMed: 27258660]
21. Garg M; Dalela D; Dalela D; Goel A; Kumar M; Gupta G; Sankhwar SN, Selective estrogen receptor modulators for BPH: new factors on the ground. Prostate Cancer Prostatic Dis 2013, 16, (3), 226–32. [PubMed: 23774084]
22. Nicholson TM; Ricke WA, Androgens and estrogens in benign prostatic hyperplasia: past, present and future. Differentiation 2011, 82, (4–5), 184–99. [PubMed: 21620560]
23. Nicholson TM; Moses MA; Uchtmann KS; Keil KP; Bjorling DE; Vezina CM; Wood RW; Ricke WA, Estrogen receptor-alpha is a key mediator and therapeutic target for bladder complications of benign prostatic hyperplasia. J Urol 2015, 193, (2), 722–9. [PubMed: 25167991]
24. Nicholson TM; Ricke EA; Marker PC; Miano JM; Mayer RD; Timms BG; vom Saal FS; Wood RW; Ricke WA, Testosterone and 17beta-estradiol induce glandular prostatic growth, bladder outlet obstruction, and voiding dysfunction in male mice. Endocrinology 2012, 153, (11), 5556–65. [PubMed: 22948219]
25. Keil KP; Abler LL; Altmann HM; Wang Z; Wang P; Ricke WA; Bjorling DE; Vezina CM, Impact of a folic acid-enriched diet on urinary tract function in mice treated with testosterone and estradiol. Am J Physiol Renal Physiol 2015, 308, (12), F1431–43. [PubMed: 25855514]
26. Erde J; Loo RR; Loo JA, Enhanced FASP (eFASP) to increase proteome coverage and sample recovery for quantitative proteomic experiments. J Proteome Res 2014, 13, (4), 1885–95. [PubMed: 24552128]
27. Cox J; Mann M, MaxQuant enables high peptide identification rates, individualized p.p.b.range mass accuracies and proteome-wide protein quantification. Nat Biotechnol 2008, 26, (12), 1367–72. [PubMed: 19029910]
28. Tyanova S; Temu T; Sinitcyn P; Carlson A; Hein MY; Geiger T; Mann M; Cox J, The Perseus computational platform for comprehensive analysis of (prote)omics data. Nat Methods 2016, 13, (9), 731–40. [PubMed: 27348712]
29. Shannon P; Markiel A; Ozier O; Baliga NS; Wang JT; Ramage D; Amin N; Schwikowski B; Ideker T, Cytoscape: a software environment for integrated models of biomolecular interaction networks. Genome Res 2003, 13, (11), 2498–504. [PubMed: 14597658]

30. Maere S; Heymans K; Kuiper M, BiNGO: a Cytoscape plugin to assess overrepresentation of gene ontology categories in biological networks. Bioinformatics 2005, 21, (16), 3448–9. [PubMed: 15972284]

31. Chen GY; Nunez G, Sterile inflammation: sensing and reacting to damage. Nat Rev Immunol 2010, 10, (12), 826–37. [PubMed: 21088683]

32. Rubartelli A; Lotze MT, Inside, outside, upside down: damage-associated molecular-pattern molecules (DAMPs) and redox. Trends Immunol 2007, 28, (10), 429–36. [PubMed: 17845865]

33. Nickel JC; Roehrborn CG; O'Leary MP; Bostwick DG; Somerville MC; Rittmaster RS, The relationship between prostate inflammation and lower urinary tract symptoms: examination of baseline data from the REDUCE trial. Eur Urol 2008, 54, (6), 1379–84. [PubMed: 18036719]

34. Minciullo PL; Inferrera A; Navarra M; Calapai G; Magno C; Gangemi S, Oxidative stress in benign prostatic hyperplasia: a systematic review. Urol Int 2015, 94, (3), 249–54. [PubMed: 25503259]

35. Thomas S; Hao L; Ricke WA; Li L, Biomarker discovery in mass spectrometry-based urinary proteomics. Proteomics Clin Appl 2016, 10, (4), 358–70. [PubMed: 26703953]

36. Hao L; Thomas S; Greer T; Vezina CM; Bajpai S; Ashok A; De Marzo AM; Bieberich CJ; Li L; Ricke WA, Quantitative proteomic analysis of a genetically induced prostate inflammation mouse model via custom 4-plex DiLeu isobaric labeling. Am J Physiol Renal Physiol 2019, 316, (6), F1236–F1243. [PubMed: 30995113]

37. Robinette CL, Sex-hormone-induced inflammation and fibromuscular proliferation in the rat lateral prostate. Prostate 1988, 12, (3), 271–86. [PubMed: 2453862]

38. Vykhovanets EV; Resnick MI; Marengo SR, Intraprostatic Lymphocyte Profiles in Aged Wistar Rats With Estradiol Induced Prostate Inflammation. Journal of Urology 2006, 175, (4), 15341540.

39. Ellem SJ; Wang H; Poutanen M; Risbridger GP, Increased endogenous estrogen synthesis leads to the sequential induction of prostatic inflammation (prostatitis) and prostatic pre-malignancy. Am J Pathol 2009, 175, (3), 1187–99. [PubMed: 19700748]

40. Oka M; Ueda M; Oyama T; Kyotani J; Tanaka M, Effect of the phytotherapeutic agent Eviprostat on 17beta-estradiol-induced non-bacterial inflammation in the rat prostate. Prostate 2009, 69, (13), 1404–10. [PubMed: 19489033]

41. McAuley EM; Mustafi D; Simons BW; Valek R; Zamora M; Markiewicz E; Lamperis S; Williams A; Roman BB; Vezina C; Karczmar G; Oto A; Vander Griend DJ, Magnetic Resonance Imaging and Molecular Characterization of a Hormone-Mediated Murine Model of Prostate Enlargement and Bladder Outlet Obstruction. Am J Pathol 2017, 187, (11), 2378–2387. [PubMed: 28823870]

42. Santucci L; Candiano G; Petretto A; Bruschi M; Lavarello C; Inglese E; Giorgio Righetti P; Marco Ghiggeri G, From hundreds to thousands: Widening the normal human Urinome. Data Brief 2014, 1, 25–8. [PubMed: 26217681]

43. Zhao M; Li M; Yang Y; Guo Z; Sun Y; Shao C; Li M; Sun W; Gao Y, A comprehensive analysis and annotation of human normal urinary proteome. Sci Rep 2017, 7, (1), 3024. [PubMed: 28596590]

44. Vizcaino JA; Cote RG; Csordas A; Dianes JA; Fabregat A; Foster JM; Griss J; Alpi E; Birim M; Contell J; O'Kelly G; Schoenegger A; Ovelleiro D; Perez-Riverol Y; Reisinger F; Rios D; Wang R; Hermjakob H, The PRoteomics IDEntifications (PRIDE) database and associated tools: status in 2013. Nucleic Acids Res 2013, 41, (Database issue), D1063–9. [PubMed: 23203882]

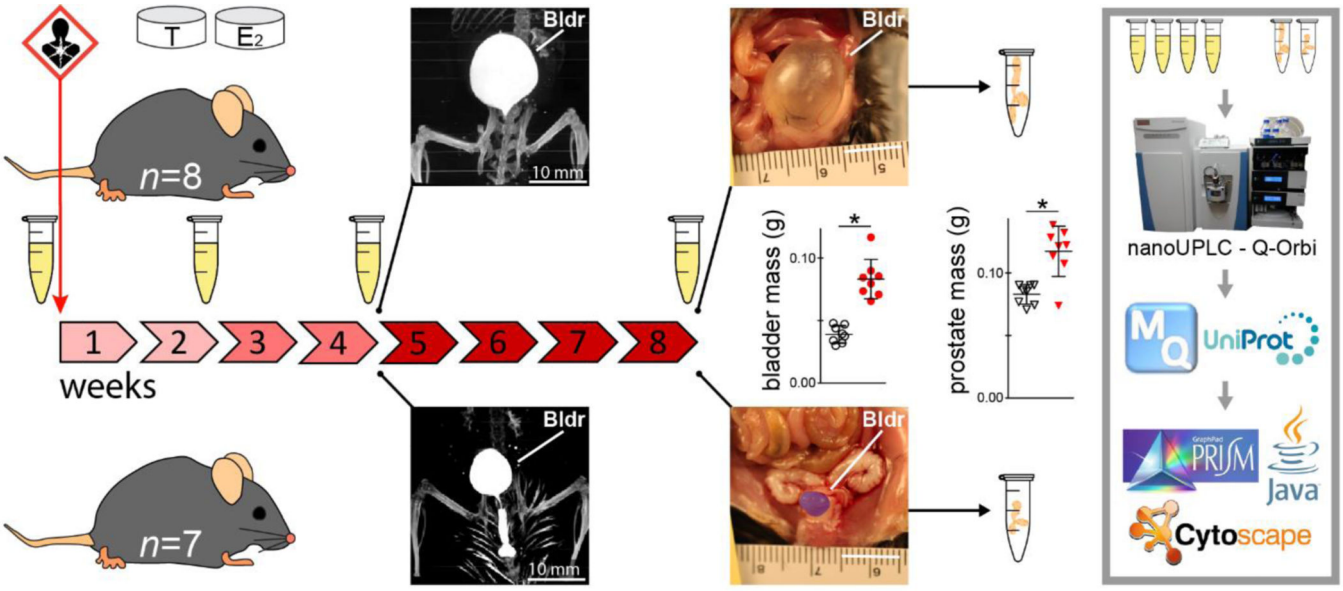

Figure 1.

Experimental design and spatiotemporal proteomics workflow. Urine samples were collected from hormone-treated mice at 4 time points: before treatment and across the development of hormone-induced bladder outlet obstruction. Bladder (Bldr) outlet obstruction was apparent by the week 4 time point via μCT imaging and marked bladder enlargement was observed at 8 weeks (control pseudocolored purple). Bladder and prostate masses at 8 weeks were significantly increased due to hormone treatment (*Student's *t*-test $p < 0.05$). Prostate tissues were collected from hormone-treated ($n = 8$) and control ($n = 7$) mice after week 8 urine collection. All urine and prostate tissue samples were analyzed for global proteomics with relative quantification via nanoUPLC-Q-Orbi.

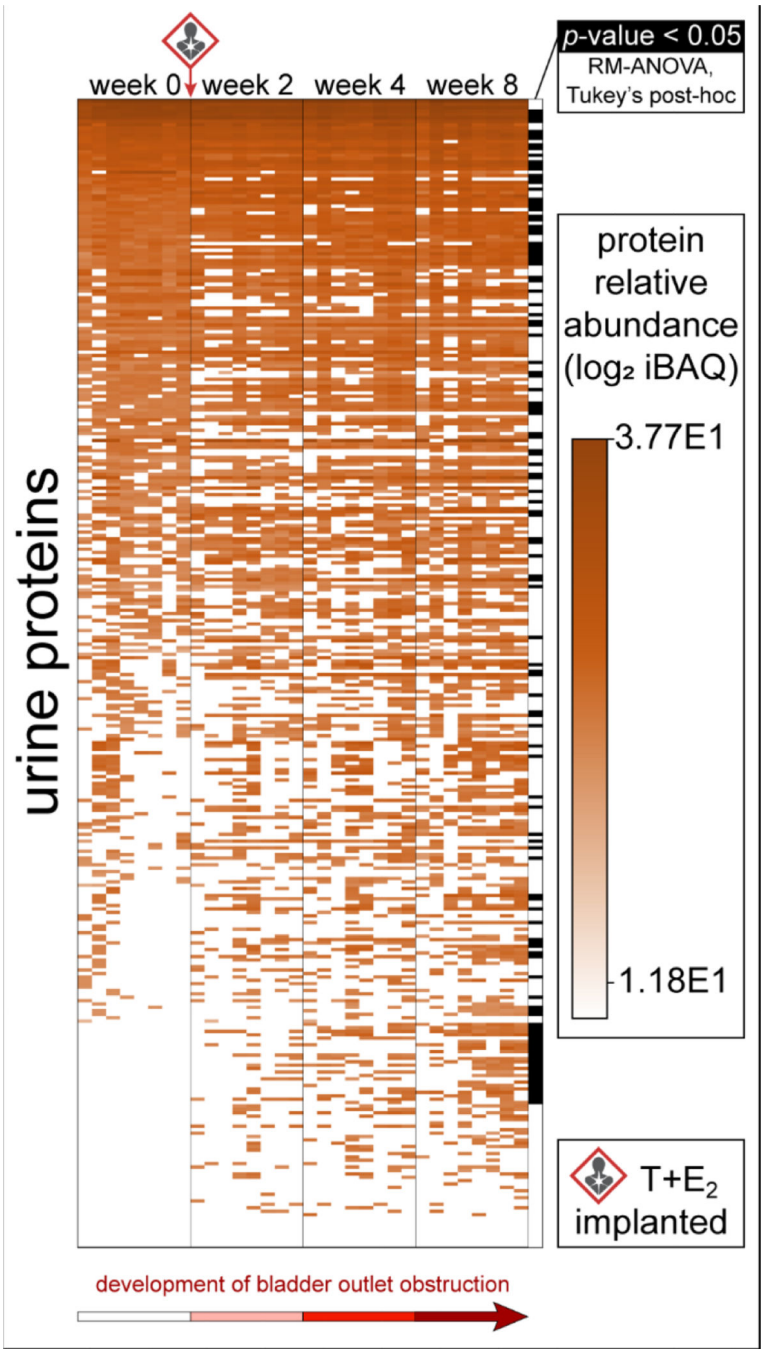

Figure 2.

Urine protein changes in hormone-treated mice across the development of bladder outlet obstruction. Heatmap of the relative protein abundance of 338 total urine protein identifications across 4 treatment time points ($n = 8$ mice); 120 of these were significantly modulated ($n = 8$; RM-ANOVA, Tukey's post-hoc test, $\alpha = 0.05$).

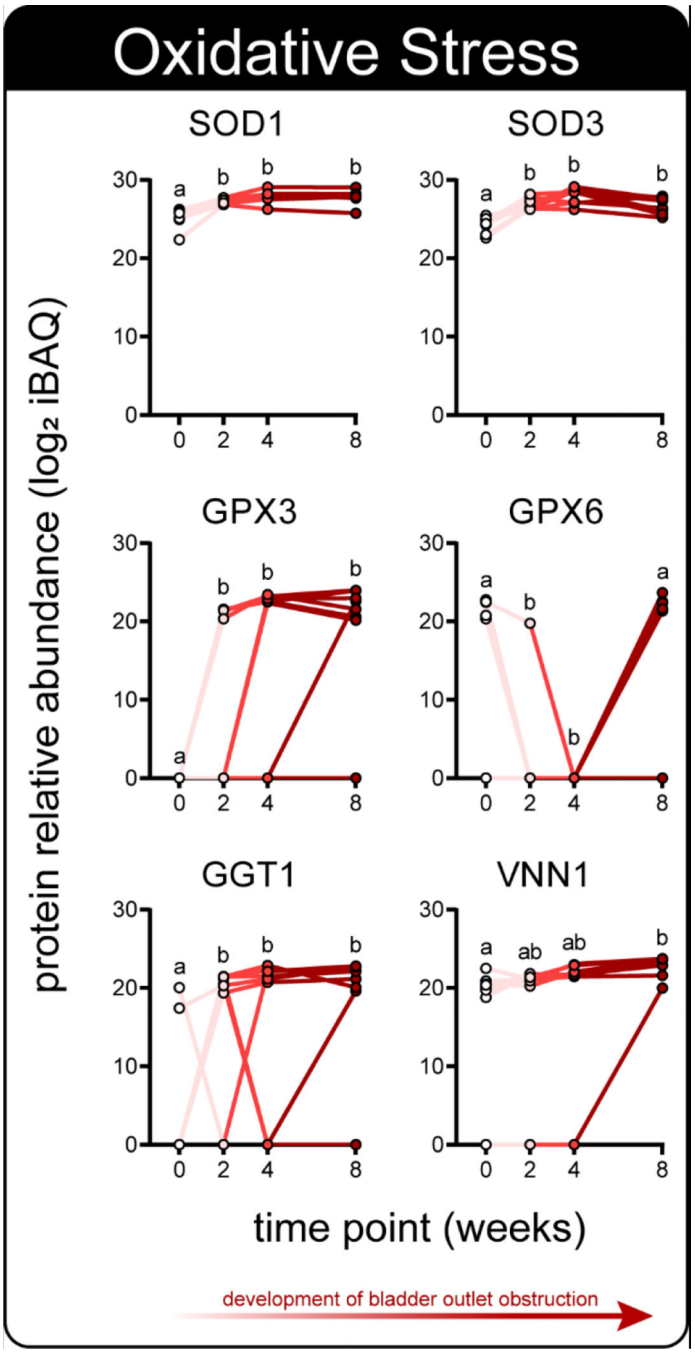

Figure 3.

A subset of significantly modulated urine proteins are related to the oxidative stress response; protein relative abundance (LFQ iBAQ) across 4 time points of disease progression. Distinct letters denote groups with significant differences ($n = 8$; RM-ANOVA, Tukey's post-hoc test, $\alpha = 0.05$).

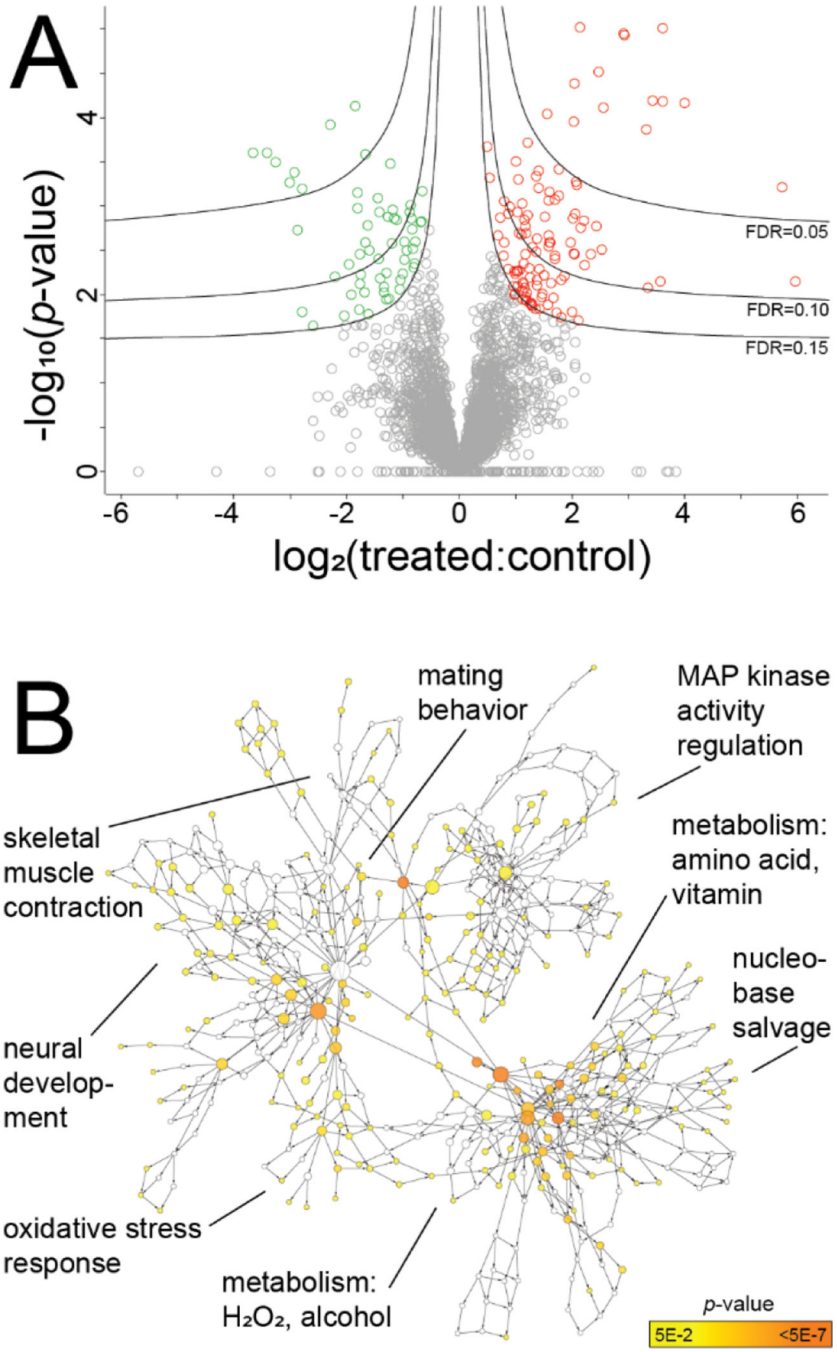

Figure 4.

Prostate tissue proteomics of hormone-treated ($n = 8$) *vs* control mice ($n = 7$). **A**: Volcano plot of 3849 total prostate proteins, 115 of which were significantly modulated (Student's *t*-test $p < 0.05$ and FDR = 0.15). **B**: Significantly enriched biological processes among these modulated proteins include the oxidative stress response, metabolism of hydrogen peroxide (H_2O_2), among others (Hypergeometric test with Benjamini & Hochberg FDR correction; Cytoscape BiNGO tool).

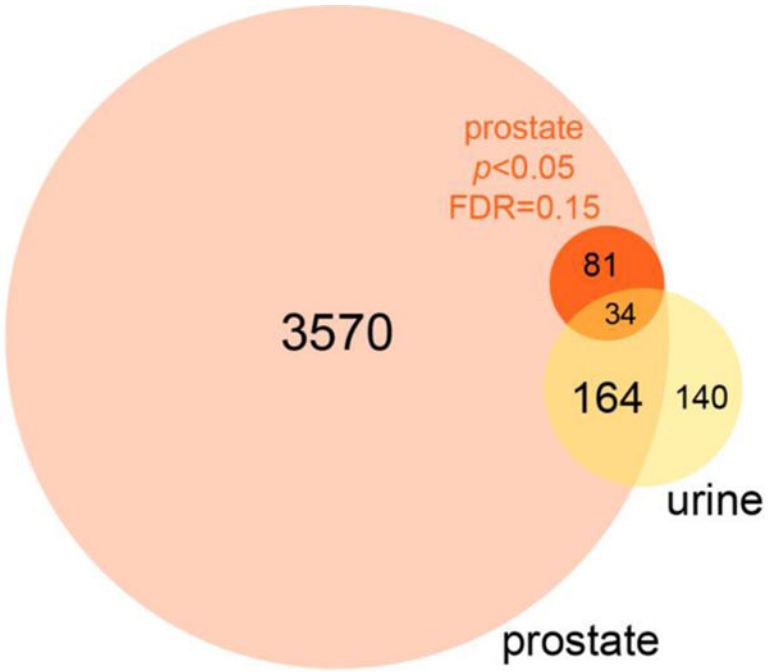

Figure 5.

Comparison of prostate and urine proteomics results for putative urinary biomarkers of hormone-induced bladder outlet obstruction. Of 3849 total prostate proteins identified, 115 were significantly modulated with hormone treatment (Student's *t*-test $p < 0.05$ and FDR = 0.15). Thirty-four of these proteins that were significantly modulated in prostate tissue coincided in urine and 15 of 34 were significantly modulated in both prostate and urine (RM-ANOVA with Tukey's post-hoc), making these putative urinary biomarkers of hormone-induced bladder outlet obstruction (see Table 1).

Table 1.

Putative urinary biomarkers of hormone treatment in the prostate; urine changes determined via RM-ANOVA with Tukey's post-hoc test, prostate changes determined via Student's *t*-test with permutation-based FDR = 0.15.

			Prostate changes	Urine changes	
Entry	**Protein name**	**Gene name**	**week 8 treated:control**	**est. change between the significant time points**	**refer to:**
P70269	Cathepsin E	*Ctse*	>10	down ~3x at week 8	Fig. S-1
P20060	Beta-hexosaminidase subunit beta	*Hexb*	4.4	up ~2x at week 8	Table S-1
P46412	Glutathione peroxidase 3	*Gpx3*	4.1	up, detectable after week 0	Fig. 3
P23953	Carboxylesterase 1C	*Ces1c*	3.4	up >10x at week 8	Fig. S-1
P09036	Serine protease inhibitor Kazal-type 1	*Spink1*	3.3	up ~4x after week 0	Fig. S-1
Q91XE4	N-acyl-aromatic-L-amino acid amidohydrolase	*Acy3*	3.1	up, detectable at week 8	Fig. S-1
P21614	Vitamin D-binding protein	*Gc*	3.0	up ~5x at week 8	Table S-1
P97449	Aminopeptidase N	*Anpep*	2.9	up ~8x at weeks 4 and 8	Fig. S-3
Q8CIF4	Biotinidase	*Btd*	2.6	up >10x at weeks 2 and 8	Table S-1
Q60928	Glutathione hydrolase 1 proenzyme	*Ggt1*	2.3	up >10x after week 0	Fig. 3
P70699	Lysosomal alpha-glucosidase	*Gaa*	2.3	up ~6x at week 4	Table S-1
P07724	Serum albumin	*Alb*	2.0	up ~3x at weeks 4 and 8	Fig. S-2
P00920	Carbonic anhydrase 2	*Ca2*	0.3	down >10x at week 8	Table S-1
Q00898	Alpha-1-antitrypsin 1–5	*Serpina1e*	0.2	down, not detected after week 0	Fig. S-1
Q9D154	Leukocyte elastase inhibitor A	*Serpinb1a*	0.2	up; detectable after week 8	Fig. S-1